Electronic Supplementary Material (ESI) for Journal of Materials Chemistry A.

Electronic Supplemental Information

Synthesis and Oxygen Evolution Reaction (OER) Catalytic Performance of $Ni_{2-x}Ru_xP$ Nanocrystals: Enhancing Activity by Dilution of the Noble Metal

*D. Ruchira Liyanage, Da Li, Quintin B. Cheek, Habib Baydoun, Stephanie L. Brock**

Department of Chemistry, Wayne State University, Detroit, Michigan 48202, United States

Attempt to synthesize Ru_xP_y nanoparticles by initial combination of $RuCl_3$ and TOP

100 mg of a Ru metal precursor was mixed with 5 mL (8.0 mmol) oleylamine, 2 mL (5.0 mmol) TOP and 10 mL octyl ether in a Schlenk flask. The system was degassed at 110 °C for 45 min followed by purging with Ar for 20 min. The system temperature was raised to 260 °C in order to form the amorphous Ru-P nanoparticles as the intermediate phase. The initial reaction mixture (dark blue) turned dark greenish after degassing and turned dark with a brownish color when the temperature was increased to 260 °C. Finally, a translucent pale brown solution was obtained, from which no solid particles could be isolated by centrifugation.

Synthesis of Ru nanoparticles

100 mg of a Ru metal precursor was mixed with 5 mL (8.0 mmol) oleylamine, and 10 mL octyl ether in a Schlenk flask. The system was degassed at 110 °C for 45 min followed by purging with Ar for 20 min. The initial color of this solution was dark blue and after the degassing step at 110 °C the color changed to pale orange. The system temperature was raised to 260 °C in order to form the Ru nanoparticles, at which point a darkening of the solution was observed. The reaction was heated for 1.5 h at 260 °C. After naturally cooling down to room temperature, ethanol was added to the flask and the solution was centrifuged to isolate the precipitate. The precipitate was dispersed again in chloroform, sonicated for 5-10 min and reprecipitated with ethanol. This sonication and precipitation process was carried out at least two times. A black precipitate was obtained as the final product and characterized by PXRD and TEM (Figure S1).

Attempt to synthesize Ru_2P nanocrystals at elevated temperatures (350 °C)

For the above-prepared Ru nanoparticles solution, the system temperature was raised to 350 °C followed by injecting 6 mL (15 mmol) of TOP. The mixture was heated at 350 °C for 4-12 h and the final product cooled to room temperature. Isolation was achieved by the procedure given for Ru nanoparticles.

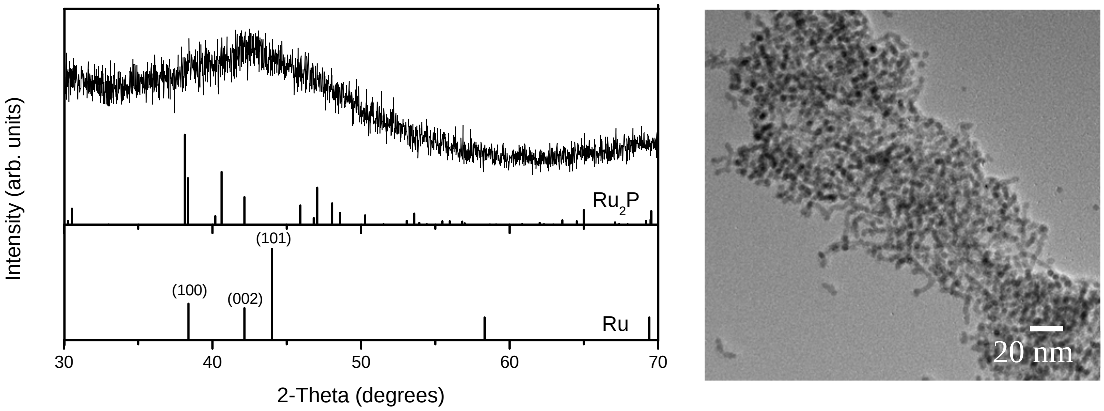

Figure S1. PXRD and TEM image of Ru nanoparticles heated at 350 °C for 12 h with 8 mL of TOP.

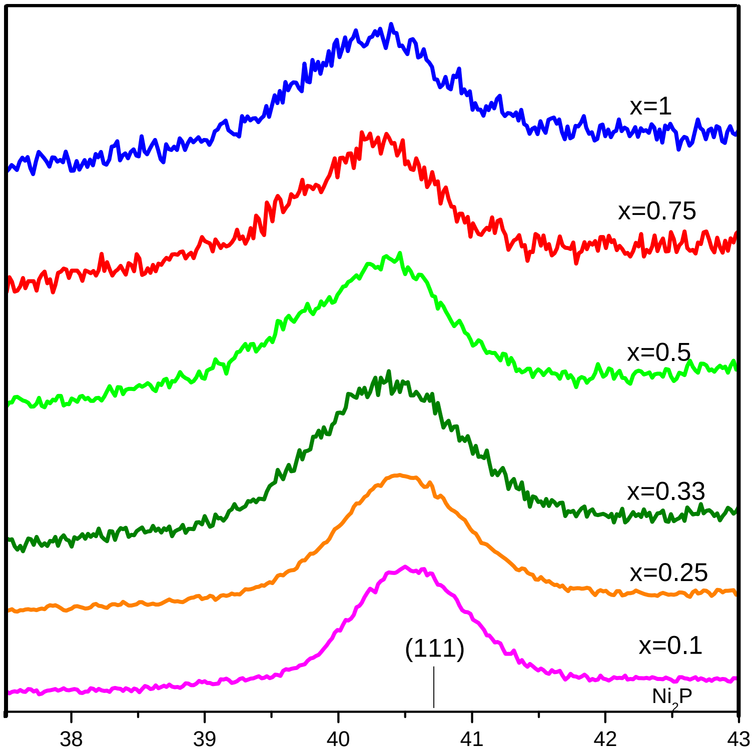

Figure S2. (111) reflection of PXRD patterns of $Ni_{2-x}Ru_xP$ calibrated against Si as an internal standard.

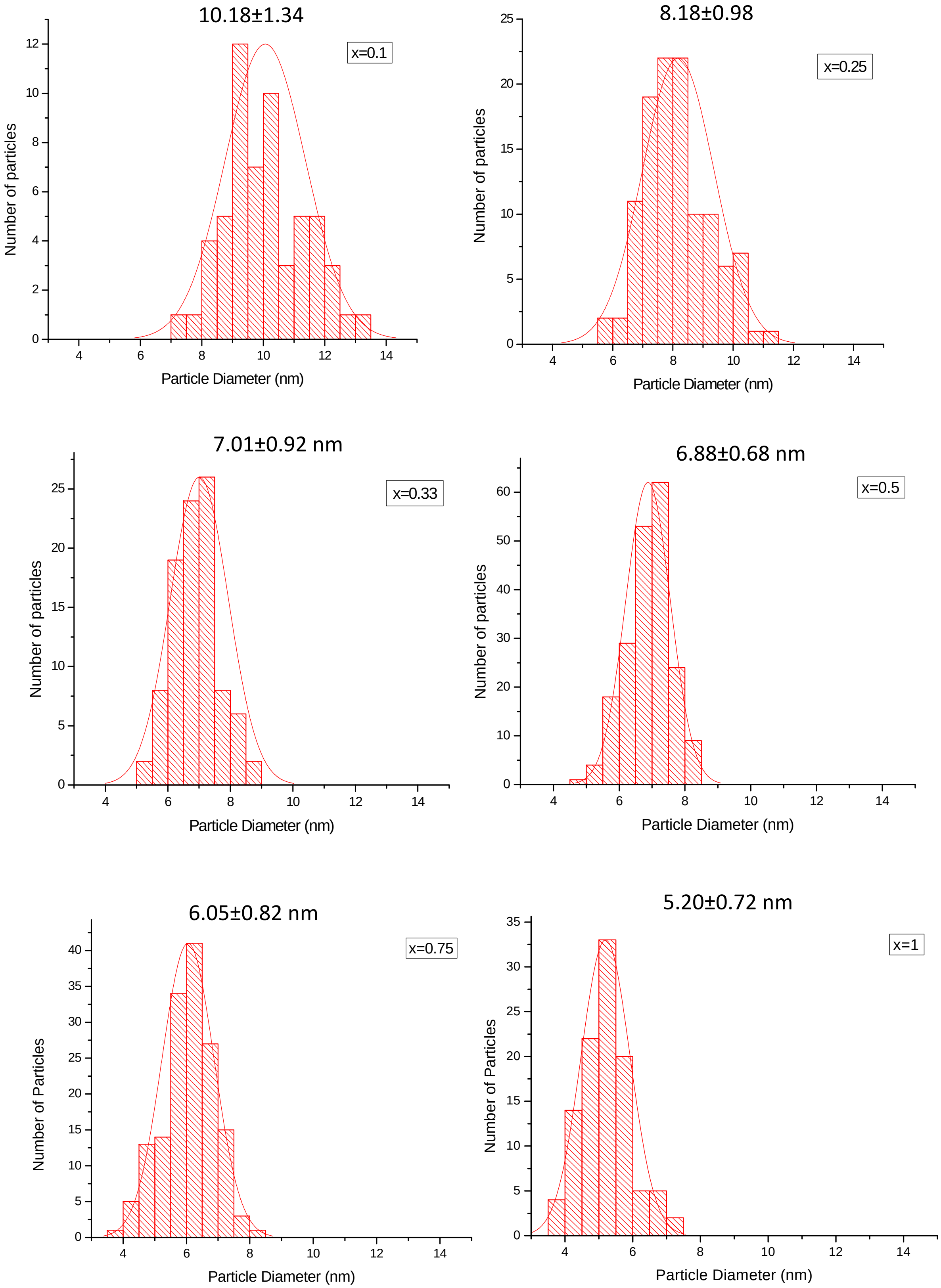

Figure S3. Particle size histograms for different $Ni_{2-x}Ru_xP$ compositions.

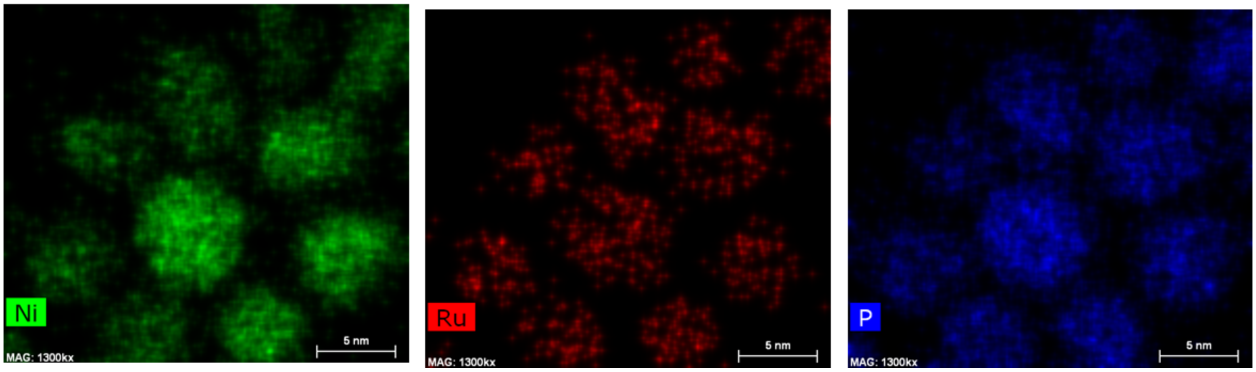

Figure S4. Elemental mapping data for few individual $Ni_{1.5}Ru_{0.5}P$ nanoparticles.

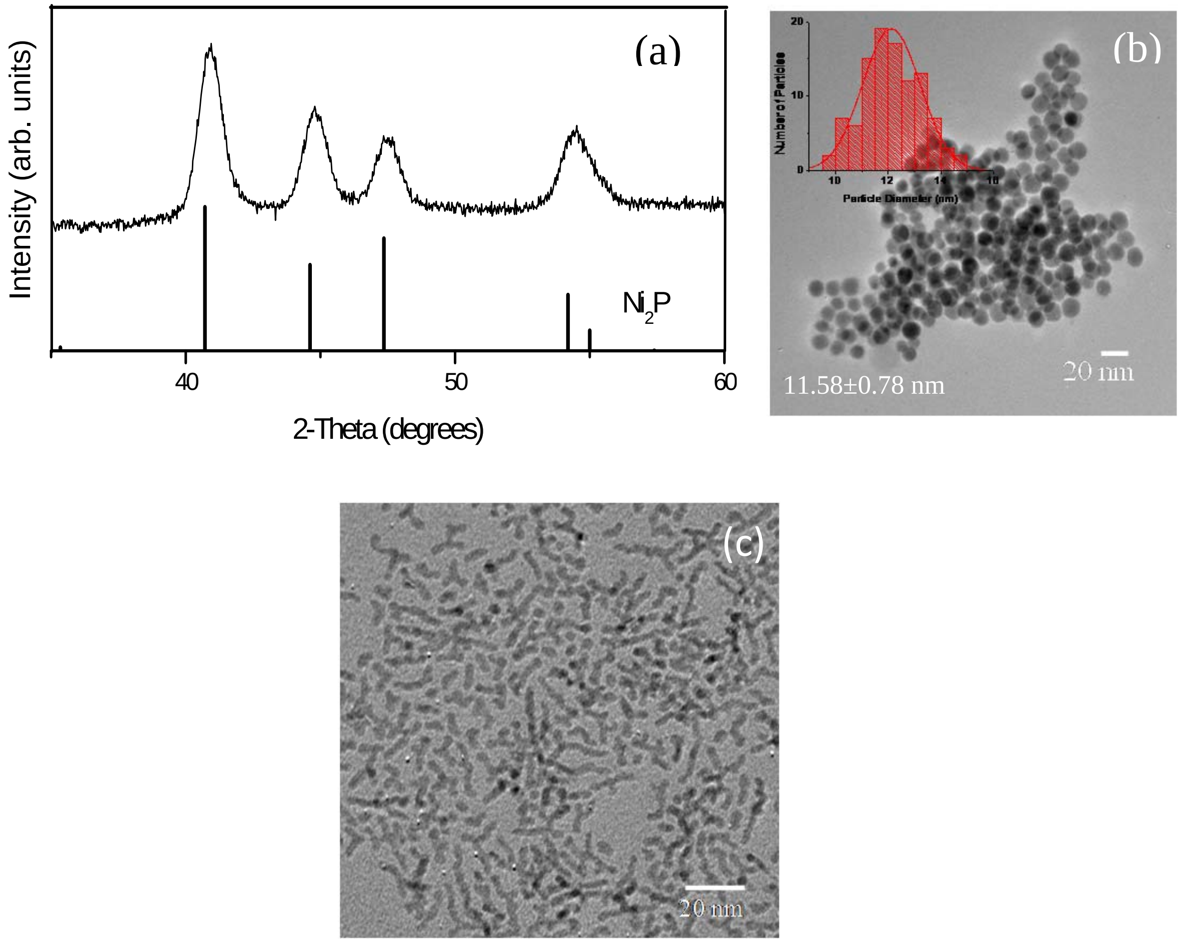

Figure S5. (a) PXRD pattern and (b) TEM image for Ni_2P particles (c) TEM image for amorphous Ru_2P particles prepared for OER catalytic testing.

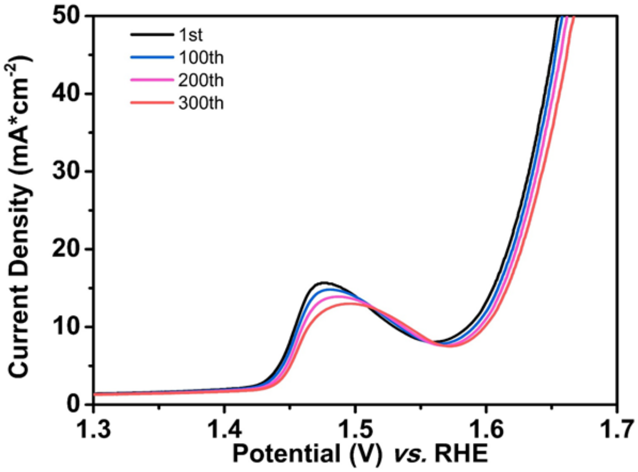

Figure S6. Polarization curves for different number of cycles of $Ni_{1.25}Ru_{0.75}P$ composition using a RDE electrode 1600 rpm in 1 M KOH.

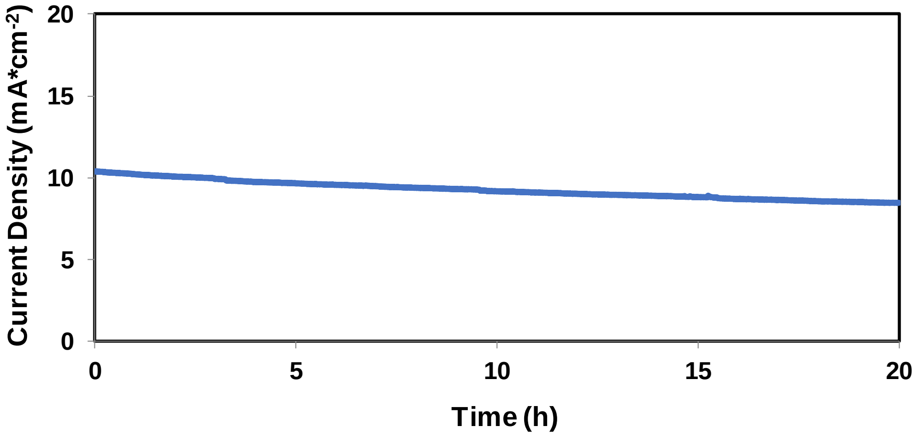

Figure S7: Chronoamperometric plot of $Ni_{1.25}Ru_{0.75}P$ composition at an applied overpotential of 0.34V using a RDE electrode at 1600 rpm in 1 M KOH.

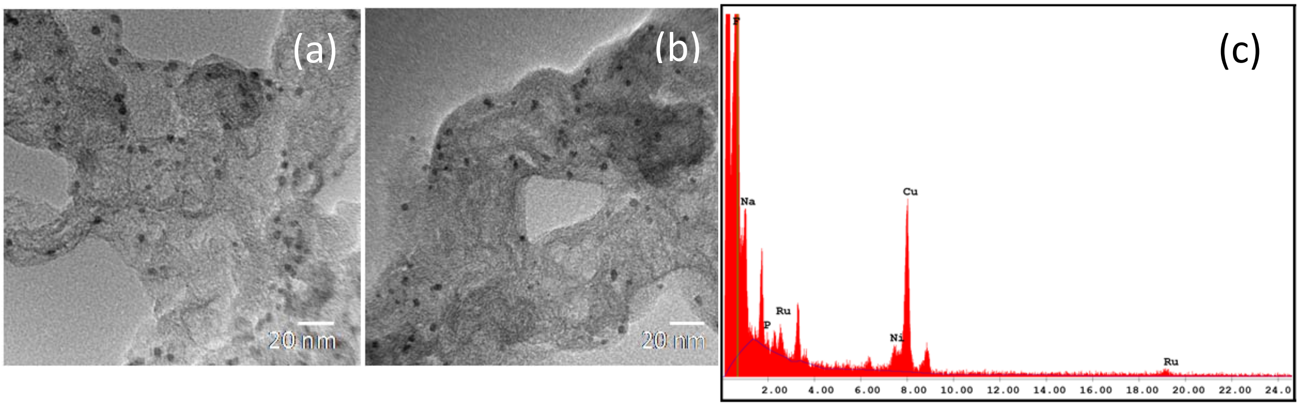

Figure S8: TEM images of $Ni_{1.25}Ru_{0.75}P$ catalyst (a) before (b) after cycle testing (c) EDS spectrum of the catalyst after cycle testing, showing that P, Ru and Ni remain. The peak at ~6.4 eV is attributed to Fe, present in the solvent in trace amounts.

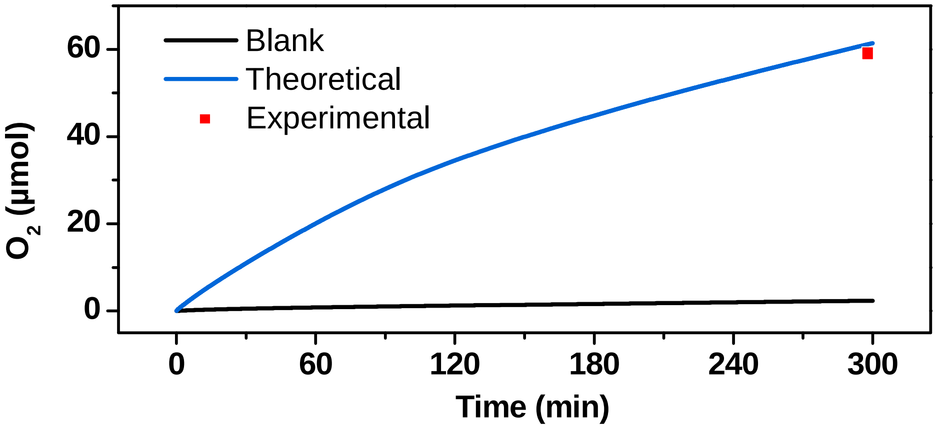

Figure S9: Faradaic efficiency: experimental vs. theoretical amount of O_2 produced

Faradaic Efficiency calculations

	% O_2	% N_2	Ratio
Air	20.3	79.7	$r_{air} = 0.2547$
Blank	20.8	79.2	$r_{blank} = 0.2626$
$Ni_{1.25}Ru_{0.75}P$	31.2	68.8	$r_{Ni1.25Ru0.75P} = 0.4535$

Head space volume = 8.5 mL

Volume of solution = 36.5 mL

Henry's law constant (K) = 769.23 $\frac{L.atm}{mol}$

nO_2 in head space before catalysis (A) = 73.79 μmol for 8.5 mL

O_2 produced in headspace = $\frac{r_{lb} - r_{blank}}{r_{air}} \times A = \frac{0.4535-0.2626}{0.2547} \times 73.79 = 55.30\ \mu mol$

O_2 dissolved = nO_2 final – nO_2 initial

$= \frac{p_{O2\,final}}{K} * V_{solution} - \frac{p_{O2\,initial}}{K} * V_{Solution}$

$= (0.312\text{-}0.203)\left(\frac{36000\ \mu L}{769.23\left(\frac{L.atm}{mol}\right)}\right) = 5.10\ \mu mol$

Total amount of O_2 produced = n_{O2} in headspace + n_{O2} dissolved

= 55.30 + 5.10

= 60.40 μmol

nO_2 based on charge = $\frac{Q_{LB} - Q_{blank}}{4 \times 0.096485} = \frac{24.612-0.913}{4 \times 0.096485} = 61.41\ \mu mol$

Faradaic efficiency = $\frac{n_{O2\,experimental}}{n_{O2\,charge}} \times 100 = \frac{60.40}{61.41} \times 100 = 98\ \%$

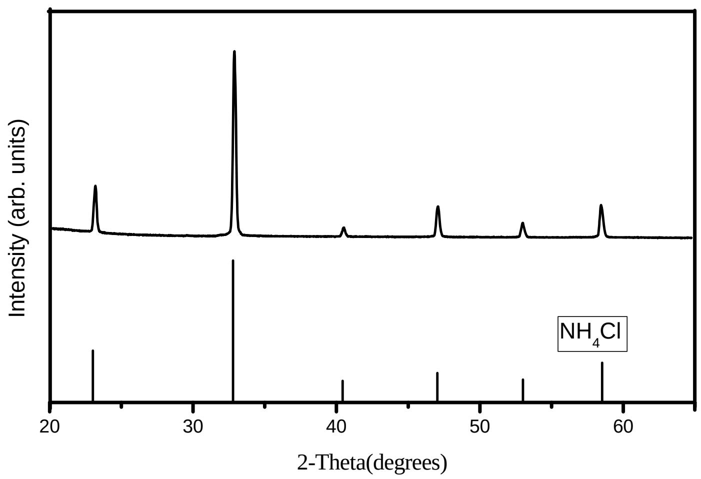

Figure S10. PXRD pattern of the by-product collected from the neck of the flask after syntheses of $Ni_{2-x}Ru_xP$ and reference PDF for NH_4Cl.

Table S1. Comparison of overpotential data for traditional RuO_2 and IrO_2 OER catalysts and recent noble metal, and noble metal phosphide, OER catalysts

Material	Overpotential (mV)	Electrolyte	Reference
RuO_2	370 mV (at 10 mA/cm^2)	1M KOH	1
RuO_2	370 mV (at 10 mA/cm^2)	0.1 M KOH	2
IrO_2	320 mV (at 10 mA/cm^2)	1M KOH	3
IrO_2	360 mV (at 10 mA/cm^2)	1M KOH	4
IrO_2	470 mV (at 10 mA/cm^2)	0.1 M KOH	5
Rh_2P nanocubes/C	510 mV (at 5 mA/cm^2)	0.5 M H_2SO_4	6
Rh/C	560 mV (at 5 mA/cm^2)	0.5 M H_2SO_4	6
Pt/C	630 mV (at 5 mA/cm^2)	0.5 M H_2SO_4	6

Table S2. Composition of the electrolyte before and after the cycle testing for $Ni_{1.25}Ru_{0.75}P$.

Element	KOH (ppb)	Soak (ppb)	After catalytic cycles (ppb)
P	8.5	11.6	326.6
Ni	19.1	18	3.2
Ru	0	2.08	57.4
Fe	29.8	22.32	19.7

References:

(1) Li, D.; Baydoun, H.; Kulikowski, B.;Brock, S. L. *Chem. Mater.* 2017**, 29,** 3048-3054.

(2) Gao, M.-R.; Cao, X.; Gao, Q.; Xu, Y.-F.; Zheng, Y.-R.; Jiang, J.; Yu, S.-H. *ACS Nano* 2014**, 8,** 3970-3978.

(3) McCrory, C. C. L.; Jung, S.; Peters, J. C.; Jaramillo, T. F. *J. Am. Chem. Soc.* 2013, **135**, 16977-16987.

(4) Dutta, A.; Samantara, A. K.; Dutta, S. K.; Jena, B. K.; Pradhan, N. *ACS Energy Lett.* 2016, **1**, 169-174.

(5) Lee, Y.; Suntivich, J.; May, K. J.; Perry, E. E.; Shao-Horn, Y. *J. Phys. Chem. Lett.* 2012, **3**, 399-404.

(6) Duan, H.; Li, D.; Tang, Y.; He, Y.; Ji, S.; Wang, R.; Lv, H.; Lopes, P. P.; Paulikas, A. P.; Li, H.; Mao, S. X.; Wang, C.; Markovic, N. M.; Li, J.; Stamenkovic, V. R.;Li, Y. *J. Am. Chem. Soc.* 2017**, 139**, 5494-5502.